ChemComm

In-situ synthesis of a high-performance bismuth oxide based composite cathode for low temperature solid oxide fuel cells

Journal:	*ChemComm*
Manuscript ID	CC-COM-01-2019-000442.R1
Article Type:	Communication

Chemical Communications

COMMUNICATION

In-situ synthesis of a high-performance bismuth oxide based composite cathode for low temperature solid oxide fuel cells

Wei Fang,*[ab] Tianrang Yang,[a] and Kevin Huang*[a]

Received 00th January 20xx,
Accepted 00th January 20xx

DOI: 10.1039/x0xx00000x

www.rsc.org/

Here, we report the design and fabrication of a cost-effective and high-performance composite $(Bi_{0.75}Y_{0.25})_{0.93}Ce_{0.07}O_{1.5\pm\delta}$-$La_{0.8}Sr_{0.2}MnO_3$ cathode by in-situ synthesis strategy with single-step phase formation and microstructure assembly, which shows lower cathode polarization resistance and better oxygen reduction reaction activity than the conventional LSM-based cathodes for low temperature solid oxide fuel cells.

Solid oxide fuel cells (SOFCs) have garnered much attention as a promising candidate power generator in the past few decades due to their high energy conversion efficiency, unique fuel flexibility and low emissions.[1] However, the commercial deployment of SOFCs has been seriously impeded by their low operating reliability (e.g. poor durability and thermal cycling) and high system cost.[2] One possible route to mitigate these problems is lowering the operation temperature of SOFCs, which can find applications in both large-scale and distributed power markets.[3]

Generally speaking, achieving high performance of SOFCs at low temperatures (LT, below 650 °C) needs to lower the resistance of electrolytes (such as reducing the thickness of electrolytes or employing the highly conductive electrolytes) and enhance the rate of oxygen reduction reaction (ORR) at cathodes.[4] Owing to a combination of fast oxygen-ion mobility and good chemical stability under reducing atmospheres, fluorite-type doped CeO_2 have been extensively studied as one of the state-of-the-art electrolytes.[5] On the other hand, most of the well-established cathode materials for SOFCs are mixed ionic-electronic conducting perovskite oxides, for example, $Ba_{0.5}Sr_{0.5}Co_{0.8}Fe_{0.2}O_{3-\delta}$,[6] $La_{1-x}Sr_xCo_{1-y}Fe_yO_{3-\delta}$.[7] However, these perovskites suffer from the phase-transformation induced performance degradation at low temperatures[8] and thermal incompatibility with most widely used electrolytes (such as Gd-doped CeO_2, GDC or Y-stabilized ZrO_2, YSZ) because of their greatly different thermal expansion coefficients.[9] Additionally, their practical applications could be also limited by long-term stability due to Sr segregation[10] and CO_2 poisoning.[11] In contrast, composite cathodes could alleviate the above drawbacks by combining pure oxygen-ionic conducting materials with pure electronic conducting materials.[12]

Conventional perovskite-type Sr-doped $LaMnO_3$ (LSM) have been historically used as an electronic conductor in the composite cathode (a mixture of electrolyte and LSM) of SOFCs, owing to its high structural/chemical stability and suitable compatibility with YSZ/GDC electrolyte.[13] On the other hand, stabilized fluorite-type Bi_2O_3 exhibits the highest oxygen-ionic conductivity under the oxidizing atmospheres among all the well-known oxide-ion conductors.[14] For example, Er-stabilized Bi_2O_3 (ESB) shows exceptionally high conductivity at 500 °C (0.0268 S cm^{-1}), which is much higher than that of YSZ (0.0009 S cm^{-1}) and GDC (0.005 S cm^{-1}).[3a,14b,15] Unfortunately, the conductivity of ESB is not stable, degrading by 25 times after annealing at 500 °C for 100 h; the degradation is found to result from the order-disorder transition of oxygen vacancies or phase transformation.[14c] To improve the stability of Bi_2O_3-based oxides, aliovalent doping with rare earth cations have been systematically investigated by Wachsman et. al.[16] By co-doping Y and Ce into Bi_2O_3, a relatively high and stable ionic conductivity of 0.008 S cm^{-1} was achieved at 500 °C for 100 h.[14c] Therefore, combining co-doped Bi_2O_3 oxygen-ion conductor with LSM as a composite cathode for LT-SOFCs is a logical choice.

Very recently, the one-pot method has proved to be applicable for preparing the composite materials with highly elaborate morphologies and unique properties.[17] We herein report the synthesis of Bi_2O_3-based and LSM composite with the modified one-pot method. The detail compositions of choice for the materials are $(Bi_{0.75}Y_{0.25})_{0.93}Ce_{0.07}O_{1.5\pm\delta}$(BYC) and $La_{0.8}Sr_{0.2}MnO_3$(LSM), respectively. The study also focuses on

[a] Department of Mechanical Engineering, University of South Carolina, Columbia, 29208, USA. E-mail: huang46@cec.sc.edu
[b] School of Materials Science and Engineering, Nanyang Technological University, 639798, Singapore. E-mail: fangwei@ntu.edu.sg
Electronic Supplementary Information (ESI) available: [details of any supplementary information available should be included here]. See DOI: 10.1039/x0xx00000x

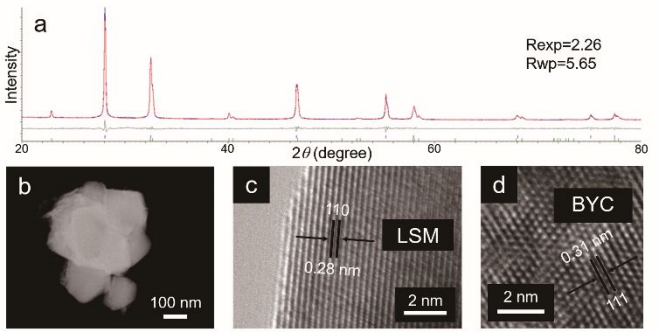

Fig. 1 a) Refined XRD pattern and b) STEM micrograph of as-synthesized in-situ BYC-LSM powders. HRTEM micrographs of c) LSM phase and d) BYC phase.

understanding the phase-assembly behaviours during synthesis (e.g. avoiding the formation of undesirable phases).

The overall synthesis route is schematically illustrated in Figure S1, where bismuth oxide, metal salts and citrate acid as gel precursors were intimately mixed, then followed by a sol-gel auto-ignition process. During the in-situ synthesis process, part of metal salts like Y and Ce enter Bi_2O_3 lattice, while the rest metal cations including La, Sr and Mn preferably self-assemble into a complex oxide with the appropriate stoichiometry. Consequently, the fluorite BYC with its adjacent perovskite LSM is successfully obtained in one single step.

In order to better understand the chemical nature of BYC-LSM composites, ambient X-ray diffraction (XRD) was applied to characterize the crystalline phases and structural compatibility of the BYC-LSM dual-phase powders. Figure 1a and Figure S2 show that LSM exhibits a rhombohedral perovskite structure with space group R-3c (PDF#00-053-0058; for in-situ powder, a=0.5514 nm, c=1.3371 nm, close to a=0.5514 nm, c=1.3366 nm of pure LSM phase), while BYC crystalizes in a cubic fluorite structure with space group Fm-3m (PDF#00-033-0223; for in-situ powder, a=0.5507, very similar to a=0.5504 nm of pure BYC phase), suggesting that high temperature δ-Bi_2O_3 phase has been stabilized to room temperature by Y- and Ce- co-doping. It is also noticed that no impurity phase is detected in the in-situ BYC-LSM composite, which suggests a good chemical compatibility between the two phases. The in-situ BYC-LSM powders were further analyzed by scanning transmission electron microscopy (STEM) and high-resolution transmission electron microscopy (HRTEM); the results are shown in Figure 1b, 1c and 1d. The d spacings of (110) and (111) planes are 0.28 and 0.31 nm respectively, close to that of rhombohedral perovskite LSM and cubic fluorite BYC, further confirming the existence of LSM and BYC phases as well.

The elemental distributions of the BYC-LSM composite powders were also investigated by energy dispersive X-ray spectroscopy (EDXS). Figure 2 of scanning electron microscopy (SEM)-EDXS and Figure S3 of transmission electron microscopy (TEM)-EDXS confirm the presence of Bi, Y, Ce, La, Sr and Mn cations in the specimens, which agrees with the starting materials. Note that in comparison to the hand-mixed sample,

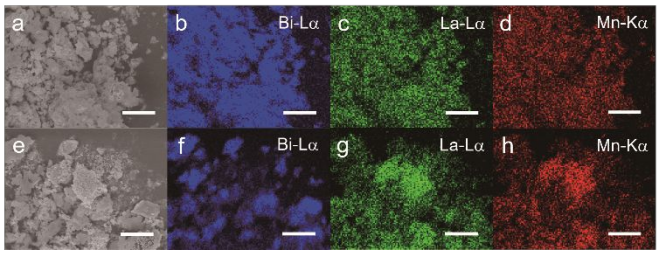

Fig. 2 Secondary electron micrographs of as-prepared a) in-situ BYC-LSM powders and e) hand-mixed BYC-LSM powders. EDXS elemental distributions of b,f) Bi, c,g) La and d,h) Mn. Scale bar: 5 μm.

in-situ BYC-LSM powders present a higher degree of homogenization of the two phases, which is indicated by the elemental distributions (especially for Bi, La and Mn). Therefore, it is concluded that in-situ synthesis method has produced a high degree of percolation for ionic/electronic conduction, resulting in an enhanced density of triple phase boundary (TPBs) for SOFC ORR kinetics.[18]

To gain more insights into the cathode performance, the area specific resistance (ASR) measurements of the BYC-LSM composite electrodes on GDC/YSZ electrolytes were conducted in symmetrical cell configuration afterwards. The ASR of in-situ BYC-LSM cathode on GDC electrolyte depicted in Figure 3a is 19.84, 5.97, 2.13, 0.84, 0.34 and 0.14 Ω cm^2 at 500, 550, 600, 650, 700 and 750 °C, respectively. As expected, the in-situ BYC-LSM sample shows a lower ASR from 500 to 750 °C than that of hand-mixed one on GDC electrolyte. The higher ORR activity of the in-situ BYC-LSM electrode is probably derived from the continuous conduction paths of two phases, resulting in maximal TPBs.[18] However, the in-situ BYC-LSM cathode on YSZ electrolyte possesses no advantage than hand-mixed sample above 700 °C, which may be ascribed to the significant interface reaction between the cathode and electrolyte at high temperatures (e.g. higher propensity for the formation of low-conductivity $La_2Zr_2O_7$ or $SrZrO_3$ phases).[19] Specially, for LT-SOFC application, the ASR of in-situ BYC-LSM cathode prepared by screen-printing in this study is the lowest among other common composite cathodes like GDC-LSM on GDC and YSZ-LSM on YSZ.

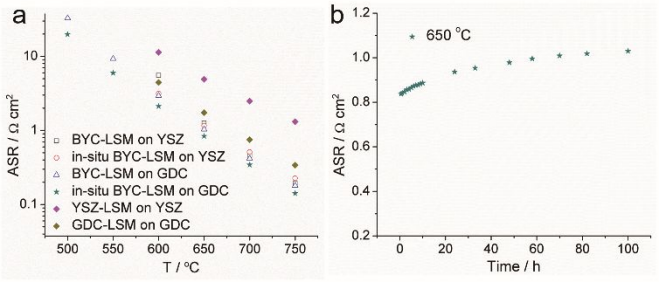

Fig. 3 a) Comparation of ASR of BYC-LSM with reported LSM-based composite cathode. Note that ASR values of YSZ-LSM and GDC-LSM come from ref. 12b. b) Evolution of ASR of in-situ BYC-LSM with time at 650 °C over 100 h.

The long-term ASR stability measurement of the in-situ BYC-LSM electrode was carried out subsequently. As presented in Figure 3b, a relatively stable ASR value around 1.0 Ω cm^2 over 100 h of operation at 650 °C is achieved for the in-situ BYC-LSM cathode on GDC electrolyte, demonstrating a good chemical compatibility between BYC-LSM and GDC. The time "aging" effect on ASR is attributed to the deactivation of oxygen dissociative adsorption on the cathode surface.[20]

Based on the above findings, anode supported SOFCs, see Figure S4, were fabricated to further evaluate the performance of BYC-LSM composite cathodes by in-situ synthesis and hand-mixing methods, together with Ni-GDC and GDC as anode and electrolyte respectively. Figure 4a presents the current-voltage and current-power plots of the single cell by employing in-situ BYC-LSM cathode. The cell open circuit voltage at 500, 550, 600 and 650 °C is 0.95, 0.94, 0.89 and 0.83 V respectively, very similar to the reported values for GDC electrolyte based SOFCs.[21] The corresponding maximum power density (MPD) is 54.8, 126.1, 280.4 and 595.6 mW cm^{-2} at 500, 550, 600 and 650 °C, respectively. It is worth noting that the MPD by using hand-mixed cathode is ~50% lower than in-situ cathode on the same electrolyte and anode (Figure 4b). The impedance spectra of the single cell with in-situ BYC-LSM cathode at 500-650 °C are shown in Figure 4c. Both the ohmic resistance and electrode (anode+cathode) polarization resistance significantly decrease with increasing the temperatures. Moreover, the obviously higher electrode polarization resistances are observed for hand-mixed cathode (Figure 4d). These results further imply a much better electrocatalytic activity of in-situ BYC-LSM than hand-mixed one towards ORR. In addition, since the ohmic resistance is usually one order of magnitude lower than the electrode polarization resistance, reducing the cathode polarization resistance will consider to be the most effective way to enhance the performance of LT-SOFCs.

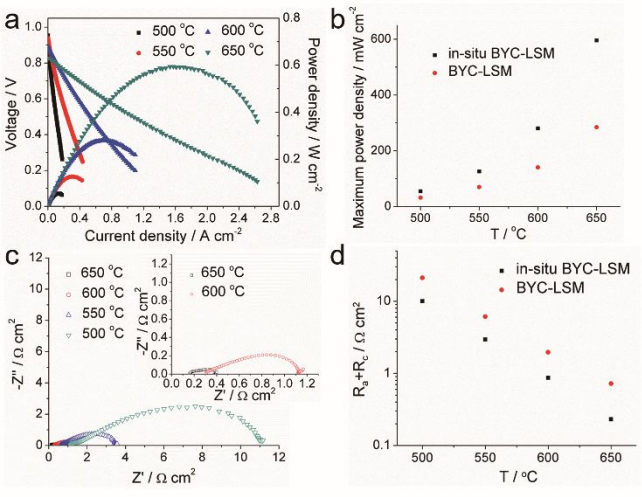

Fig. 4 a) Current-voltage and current-power curves and c) electrochemical impedance spectra of anode supported SOFC with in-situ BYC-LSM cathode. Comparisons of b) maximum power density and d) electrode resistances of SOFCs with different BYC-LSM composite cathodes. Thickness of GDC electrolyte: ~40 μm.

In summary, a composite cathode for LT-SOFC with high activity and good stability was successfully developed by a facile in-situ synthesis approach. It is further demonstrated that the percolation behaviors, which is omnipresent in composite conducting materials, has a significant impact on the electrocatalytic activity for oxygen reduction reaction. Thus, it is reasonable to expect that the proper in-situ synthesis method can produce high-performance composite electrodes with exceptional percolation for low temperature applications.

Conflicts of interest

There are no conflicts to declare.

Notes and references

1 a) M. Liu, M. E. Lynch, K. Blinn, F. M. Alamgir, Y. Choi, *Mater. Today*, 2011, **14**, 534; b) S. W. Tao, J. T. S. Irvine, *Nat. Mater.*, 2003, **2**, 320; c) H. Kim, J. M. Vohs, R. J. Gorte, *Chem. Commun.*, 2001, 2334.
2 a) R. O'Hayre, S. W. Cha, W. G. Colella, F. B. Prinz, *Fuel Cell Fundamentals*, Wiley, New York, 2009; b) A. B. Stambouli, E. Traversa, *Renew. Sust. Energ. Rev.*, 2002, **6**, 433.
3 a) E. D. Wachsman, K. T. Lee, *Science*, 2011, **334**, 935; b) Z. Gao, L. V. Mogni, E. C. Miller, J. G. Railsback, S. A. Barnett, *Energy Environ. Sci.*, 2016, **9**, 1602; c) Y. Zhang, R. Knibbe, J. Sunarso, Y. J. Zhong, W. Zhou, Z. P. Shao, Z. H. Zhu, *Adv. Mater.*, 2017, **29**, 1700132.
4 a) S. Yoo, A. Jun, Y. W. Ju, O. Odkhuu, J. Hyodo, H. Y. Jeong, N. Park, J. Shin, T. Ishihara, G. Kim, *Angew. Chem. Int. Ed.*, 2014, **53**, 13064; b) J. G. Lee, J. H. Park, Y. G. Shul, *Nat. Commun.*, 2014, **5**, 4045; c) B. Hua, Y. Q. Zhang, N. Yan, M. Li, Y. F. Sun, J. Chen, J. Li, J. L. Luo, *Adv. Funct. Mater.*, 2016, **26**, 4106.
5 a) M. Mogensen, N. M. Sammes, G. A. Tompsett, *Solid State Ionics*, 2000, **129**, 63; b) V. V. Kharton, F. M. Figueiredo, L. Navarro, E. N. Naumovich, A. V. Kovalevsky, A. A. Yaremchenko, A. P. Viskup, A. Carneiro, F. M. B. Marques, J. R. Frade, *J. Mater. Sci.*, 2001, **36**, 1105; c) S. J. Skinner, J. A. Kilner, *Mater. Today*, 2003, **6**, 30.
6 a) Z. P. Shao, S. M. Haile, *Nature*, 2004, **431**, 170; b) W. Zhou, R. Ran, Z. P. Shao, *J. Power Sources*, 2009, **192**, 231.
7 a) A. Petric, P. Huang, F. Tietz, *Solid State Ionics*, 2000, **135**, 719; b) L. Qiu, T. Ichikawa, A. Hirano, N. Imanishi, Y. Takeda, *Solid State Ionics*, 2003, **158**, 55.
8 a) D. N. Mueller, R. A. De Souza, T. E. Weirich, D. Roehrens, J. Mayer, M. Martin, *Phys. Chem. Chem. Phys.*, 2010, **12**, 10320; b) P. Müller, H. Störmer, M. Meffert, L. Dieterle, C. Niedrig, S. F. Wagner, E. I. Tiffée, D. Gerthsen, *Chem. Mater.*, 2013, **25**, 564.
9 a) F. Tietz, *Ionics*, 1999, **5**, 129; b) E. V. Tsipis, V. V. Kharton, *J. Solid State Electrochem.*, 2008, **12**, 1367.
10 a) S. P. Simner, M. D. Anderson, M. H. Engelhard, J. W. Stevenson, *Electrochem. Solid-State Lett.*, 2006, **9**, A478; b) W. C. Jung, H. L. Tuller, *Energy Environ. Sci.*, 2012, **5**, 5370.
11 a) A. Y. Yan, M. J. Cheng, Y. L. Dong, W. S. Yang, V. Maragou, S. Q. Song, P. Tsiakaras, *Appl. Catal. B: Environ.*, 2006, **66**, 64; b) E. Bucher, A. Egger, G. B. Caraman, W. Sitte, *J. Electrochem. Soc.*, 2008, **155**, B1218.
12 a) M. J. Jørgensen, M. Mogensen, *J. Electrochem. Soc.*, 2001, **148**, A433; b) E. P. Murray, S. A. Barnett, *Solid State Ionics*, 2001, **143**, 265.
13 a) San Ping Jiang, *J. Mater. Sci.*, 2008, **43**, 6799; b) M. Balaguer, V. B. Vert, L. Navarrete, J. M. Serra, *J. Power Sources*, 2013,

223, 214; c) L. Liu, Z. Zhao, X. M. Zhang, D. A. Cui, B. F. Tu, D. R. Ou, M. J. Cheng, *Chem. Commun.*, 2013, **49**, 777.

14 a) P. Shuk, H. D. Wiemhöfer, U. Guth, W. Göpel, M. Greenblatt, *Solid State Ionics*, 1996, **89**, 179; b) K. T. Lee, A. A. Lidie, H. S. Yoon, E. D. Wachsman, *Angew. Chem. Int. Ed.*, 2014, **53**, 13463; c) C. J. Zhang, K. Huang, *J. Power Sources*, 2017, **342**, 419.

15 a) C. D. Zuo, S. W. Zha, M. L. Liu, M. Hatano, M. Uchiyama, *Adv. Mater.*, 2006, **18**, 3318; b) J. W. Fergus, *J. Power Sources*, 2006, **162**, 30.

16 a) D. W. Jung, K. L. Duncan, E. D. Wachsman, *Acta Mater.*, 2010, **58**, 355; b) A. L. Ruth, K. T. Lee, M. Clites, E. D. Wachsman, *ECS Trans.*, 2014, **64**, 135; c) A. Pesaran, A. Jaiswal, Y. Y. Ren, E. D. Wachsman, *Ionics*, 2019, https://doi.org/10.1007/s11581-019-02838-4.

17 a) W. Fang, C. Zhang, F. Steinbach, A. Feldhoff, *Angew. Chem. Int. Ed.*, 2017, **56**, 7584; b) F. S. Li, L. Jiang, R. Zeng, T. Wei, F. Wang, Y. X. Xu, Y. H. Huang, *Int. J. Hydrogen Energ.*, 2015, **40**, 12750; c) C. Jin, Y. C. Mao, D. W. Rooney, W. Sun, N. Q. Zhang, K. N. Sun, *Int. J. Hydrogen Energ.*, 2016, **41**, 4005.

18 a) P. Costamagna, P. Costa, V. Antonucci, *Electrochim. Acta*, 1998, **43**, 375; b) S. B. Adler, *Chem. Rev.*, 2004, **104**, 4791.

19 a) J. A. M. V. Roosmalen, E. H. P. Cordfunke, *Solid State Ionics*, 1992, **52**, 303; b) M. Chen, Y. L. Liu, A. Hagen, P. V. Hendriksen, F. W. Poulsen, *Fuel Cells*, 2009, **9**, 833.

20 a) Y. H. Gong, R. L. Patel, X. H. Liang, D. Palacio, X. Y. Song, J. B. Goodenough, K. Huang, *Chem. Mater.*, 2013, **25**, 4224; b) Z. H. Cai, M. Kubicek, J. Fleig, B. Yildiz, *Chem. Mater.*, 2012, **24**, 1116.

21 a) C. R. Xia, M. L. Liu, Solid State Ionics, 2001, 144, 249; b) Y. J. Leng, S. H. Chan, S. P. Jiang, K. A. Khor, Solid State Ionics, 2004, 170, 9.